

## Bottom production cross section from double muonic decays of $b$ -flavoured hadrons in 920 GeV proton-nucleus collisions

I. Abt<sup>23</sup>, M. Adams<sup>10</sup>, M. Agari<sup>13</sup>, H. Albrecht<sup>12</sup>, A. Aleksandrov<sup>29</sup>, V. Amaral<sup>8</sup>, A. Amorim<sup>8</sup>, S. J. Aplin<sup>12</sup>, V. Aushev<sup>16</sup>, Y. Bagaturia<sup>12,36</sup>, V. Balagura<sup>22</sup>, M. Bargiotti<sup>6</sup>, O. Barsukova<sup>11</sup>, J. Bastos<sup>8</sup>, J. Batista<sup>8</sup>, C. Bauer<sup>13</sup>, Th. S. Bauer<sup>1</sup>, A. Belkov<sup>11,†</sup>, Ar. Belkov<sup>11</sup>, I. Belotelov<sup>11</sup>, A. Bertin<sup>6</sup>, B. Bobchenko<sup>22</sup>, M. Böcker<sup>26</sup>, A. Bogatyrev<sup>22</sup>, G. Bohm<sup>29</sup>, M. Bräuer<sup>13</sup>, M. Bruinsma<sup>28,1</sup>, M. Bruschi<sup>6</sup>, P. Buchholz<sup>26</sup>, T. Buran<sup>24</sup>, J. Carvalho<sup>8</sup>, P. Conde<sup>2,12</sup>, C. Cruse<sup>10</sup>, M. Dam<sup>9</sup>, K. M. Danielsen<sup>24</sup>, M. Danilov<sup>22</sup>, S. De Castro<sup>6</sup>, H. Deppe<sup>14</sup>, X. Dong<sup>3</sup>, H. B. Dreis<sup>14</sup>, V. Egorytchev<sup>12</sup>, K. Ehret<sup>10</sup>, F. Eisele<sup>14</sup>, D. Emeliyanov<sup>12</sup>, S. Essenov<sup>22</sup>, L. Fabbri<sup>6</sup>, P. Faccioli<sup>6</sup>, M. Feuerstack-Raible<sup>14</sup>, J. Flammer<sup>12</sup>, B. Fominykh<sup>22</sup>, M. Funcke<sup>10</sup>, Ll. Garrido<sup>2</sup>, A. Gellrich<sup>29</sup>, B. Giacobbe<sup>6</sup>, P. Giovannini<sup>6</sup>, J. Gläß<sup>20</sup>, D. Goloubkov<sup>12,33</sup>, Y. Golubkov<sup>12,34</sup>, A. Golutvin<sup>22</sup>, I. Golutvin<sup>11</sup>, I. Gorbounov<sup>12,26</sup>, A. Gorišek<sup>17</sup>, O. Gouchtchine<sup>22</sup>, D. C. Goulart<sup>7</sup>, S. Gradl<sup>14</sup>, W. Gradl<sup>14</sup>, F. Grimaldi<sup>6</sup>, J. Groth-Jensen<sup>9</sup>, Yu. Guilitsky<sup>22,35</sup>, J. D. Hansen<sup>9</sup>, J. M. Hernández<sup>29</sup>, W. Hofmann<sup>13</sup>, M. Hohlmann<sup>12</sup>, T. Hott<sup>14</sup>, W. Hulsbergen<sup>1</sup>, U. Husemann<sup>26</sup>, O. Igonkina<sup>22</sup>, M. Ispiryan<sup>15</sup>, T. Jagla<sup>13</sup>, C. Jiang<sup>3</sup>, H. Kapitza<sup>12</sup>, S. Karabekyan<sup>25</sup>, N. Karpenko<sup>11</sup>, S. Keller<sup>26</sup>, J. Kessler<sup>14</sup>, F. Khasanov<sup>22</sup>, Yu. Kiryushin<sup>11</sup>, I. Kisel<sup>23</sup>, E. Klinkby<sup>9</sup>, K. T. Knöpfle<sup>13</sup>, H. Kolanoski<sup>5</sup>, S. Korpar<sup>21,17</sup>, C. Krauss<sup>14</sup>, P. Kreuzer<sup>12,19</sup>, P. Križan<sup>18,17</sup>, D. Krücker<sup>5</sup>, S. Kupper<sup>17</sup>, T. Kvaratskheliia<sup>22</sup>, A. Lanyov<sup>11</sup>, K. Lau<sup>15</sup>, B. Lewendel<sup>12</sup>, T. Lohse<sup>5</sup>, B. Lomonosov<sup>12,32</sup>, R. Männer<sup>20</sup>, R. Mankel<sup>29</sup>, S. Masciocchi<sup>12</sup>, I. Massa<sup>6</sup>, I. Matchikhilian<sup>22</sup>, G. Medin<sup>5</sup>, M. Medinnis<sup>12</sup>, M. Mevius<sup>12</sup>, A. Michetti<sup>12</sup>, Yu. Mikhailov<sup>22,35</sup>, R. Mizuk<sup>22</sup>, R. Muresan<sup>9</sup>, M. zur Nedden<sup>5</sup>, M. Negodaev<sup>12,32</sup>, M. Nörenberg<sup>12</sup>, S. Nowak<sup>29</sup>, M. T. Núñez Pardo de Vera<sup>12</sup>, M. Ouchrif<sup>28,1</sup>, F. Ould-Saada<sup>24</sup>, C. Padilla<sup>12</sup>, D. Peralta<sup>2</sup>, R. Pernack<sup>25</sup>, R. Pestotnik<sup>17</sup>, B. AA. Petersen<sup>9</sup>, M. Piccinini<sup>6</sup>, M. A. Pleier<sup>13</sup>, M. Poli<sup>6,31</sup>, V. Popov<sup>22</sup>, D. Pose<sup>11,14</sup>, S. Prystupa<sup>16</sup>, V. Pugatch<sup>16</sup>, Y. Pylypchenko<sup>24</sup>, J. Pyrlík<sup>15</sup>, K. Reeves<sup>13</sup>, D. Reßing<sup>12</sup>, H. Rick<sup>14</sup>, I. Riu<sup>12</sup>, P. Robmann<sup>30</sup>, I. Rostovtseva<sup>22</sup>, V. Rybnikov<sup>12</sup>, F. Sánchez<sup>13</sup>, A. Sbrizzi<sup>1</sup>, M. Schmelling<sup>13</sup>, B. Schmidt<sup>12</sup>, A. Schreiner<sup>29</sup>, H. Schröder<sup>25</sup>, U. Schwanke<sup>29</sup>, A. J. Schwartz<sup>7</sup>, A. S. Schwarz<sup>12</sup>, B. Schwenninger<sup>10</sup>, B. Schwingenheuer<sup>13</sup>, F. Sciacca<sup>13</sup>, N. Semprini-Cesari<sup>6</sup>, S. Shuvalov<sup>22,5</sup>, L. Silva<sup>8</sup>, L. Sözüer<sup>12</sup>, S. Solunin<sup>11</sup>, A. Somov<sup>12</sup>, S. Somov<sup>12,33</sup>, J. Spengler<sup>13</sup>, R. Spighi<sup>6</sup>, A. Spiridonov<sup>29,22</sup>, A. Stanovnik<sup>18,17</sup>, M. Starič<sup>17</sup>, C. Stegmann<sup>5</sup>, H. S. Subramania<sup>15</sup>, M. Symalla<sup>12,10</sup>, I. Tikhomirov<sup>22</sup>, M. Titov<sup>22</sup>, I. Tsakov<sup>27</sup>, U. Uwer<sup>14</sup>, C. van Eldik<sup>12,10</sup>, Yu. Vassiliev<sup>16</sup>, M. Villa<sup>6</sup>, A. Vitale<sup>6</sup>, I. Vukotic<sup>5,29</sup>, H. Wahlberg<sup>28</sup>, A. H. Walenta<sup>26</sup>, M. Walter<sup>29</sup>, J. J. Wang<sup>4</sup>, D. Wegener<sup>10</sup>, U. Werthenbach<sup>26</sup>, H. Wolters<sup>8</sup>, R. Wurth<sup>12</sup>, A. Wurz<sup>20</sup>, S. Xella-Hansen<sup>9</sup>, Yu. Zaitsev<sup>22</sup>, M. Zavertyaev<sup>12,13,32</sup>, T. Zeuner<sup>12,26</sup>, A. Zhelezov<sup>22</sup>, Z. Zheng<sup>3</sup>, R. Zimmermann<sup>25</sup>, T. Živko<sup>17</sup>, A. Zoccoli<sup>6</sup>

<sup>1</sup>NIKHEF, 1009 DB Amsterdam, The Netherlands <sup>a</sup>

<sup>2</sup>Department ECM, Faculty of Physics, University of Barcelona, E-08028 Barcelona, Spain <sup>b</sup>

<sup>3</sup>Institute for High Energy Physics, Beijing 100039, P.R. China

<sup>4</sup>Institute of Engineering Physics, Tsinghua University, Beijing 100084, P.R. China

<sup>5</sup>Institut für Physik, Humboldt-Universität zu Berlin, D-12489 Berlin, Germany <sup>c,d</sup>

<sup>6</sup>Dipartimento di Fisica dell' Università di Bologna and INFN Sezione di Bologna, I-40126 Bologna, Italy

<sup>7</sup>Department of Physics, University of Cincinnati, Cincinnati, Ohio 45221, USA <sup>e</sup>

<sup>8</sup>LIP Coimbra, P-3004-516 Coimbra, Portugal <sup>f</sup>

<sup>9</sup>Niels Bohr Institutet, DK 2100 Copenhagen, Denmark <sup>g</sup>

<sup>10</sup>Institut für Physik, Universität Dortmund, D-44221 Dortmund, Germany <sup>d</sup>

<sup>11</sup>Joint Institute for Nuclear Research Dubna, 141980 Dubna, Moscow region, Russia

<sup>12</sup>DESY, D-22603 Hamburg, Germany

<sup>13</sup>Max-Planck-Institut für Kernphysik, D-69117 Heidelberg, Germany <sup>d</sup>

<sup>14</sup>Physikalisches Institut, Universität Heidelberg, D-69120 Heidelberg, Germany <sup>d</sup>

<sup>15</sup>Department of Physics, University of Houston, Houston, TX 77204, USA <sup>e</sup>

<sup>16</sup>Institute for Nuclear Research, Ukrainian Academy of Science, 03680 Kiev, Ukraine <sup>h</sup>

<sup>17</sup>J. Stefan Institute, 1001 Ljubljana, Slovenia <sup>i</sup>

<sup>18</sup>University of Ljubljana, 1001 Ljubljana, Slovenia

- <sup>19</sup> *University of California, Los Angeles, CA 90024, USA* <sup>j</sup>
- <sup>20</sup> *Lehrstuhl für Informatik V, Universität Mannheim, D-68131 Mannheim, Germany*
- <sup>21</sup> *University of Maribor, 2000 Maribor, Slovenia*
- <sup>22</sup> *Institute of Theoretical and Experimental Physics, 117259 Moscow, Russia* <sup>k</sup>
- <sup>23</sup> *Max-Planck-Institut für Physik, Werner-Heisenberg-Institut, D-80805 München, Germany* <sup>d</sup>
- <sup>24</sup> *Dept. of Physics, University of Oslo, N-0316 Oslo, Norway* <sup>l</sup>
- <sup>25</sup> *Fachbereich Physik, Universität Rostock, D-18051 Rostock, Germany* <sup>d</sup>
- <sup>26</sup> *Fachbereich Physik, Universität Siegen, D-57068 Siegen, Germany* <sup>d</sup>
- <sup>27</sup> *Institute for Nuclear Research, INRNE-BAS, Sofia, Bulgaria*
- <sup>28</sup> *Universiteit Utrecht/NIKHEF, 3584 CB Utrecht, The Netherlands* <sup>a</sup>
- <sup>29</sup> *DESY, D-15738 Zeuthen, Germany*
- <sup>30</sup> *Physik-Institut, Universität Zürich, CH-8057 Zürich, Switzerland* <sup>m</sup>
- <sup>31</sup> *visitor from Dipartimento di Energetica dell' Università di Firenze and INFN Sezione di Bologna, Italy*
- <sup>32</sup> *visitor from P.N. Lebedev Physical Institute, 117924 Moscow B-333, Russia*
- <sup>33</sup> *visitor from Moscow Physical Engineering Institute, 115409 Moscow, Russia*
- <sup>34</sup> *visitor from Moscow State University, 119899 Moscow, Russia*
- <sup>35</sup> *visitor from Institute for High Energy Physics, Protvino, Russia*
- <sup>36</sup> *visitor from High Energy Physics Institute, 380086 Tbilisi, Georgia*
- † *deceased*

## Abstract

The  $b\bar{b}$  production cross section in 920 GeV proton-nucleus fixed target collisions is measured by observing double muonic decays of  $b$ -flavoured hadrons in the kinematic region  $-0.3 < x_F(\mu) < 0.15$ . A total number of  $76 \pm 12$   $b\bar{b}$  events is obtained with a likelihood fit of the signal and background simulated events to the data. The resulting cross section is  $\sigma_{b\bar{b}} = 16.2 \pm 2.5_{stat} \pm 2.8_{sys}$  nb/nucleon, or, when combined with a previous HERA-B measurement of similar precision,  $\sigma_{b\bar{b}} = 15.4 \pm 1.7_{stat} \pm 1.2_{sys}^{uncorr.} \pm 1.9_{sys}^{corr.}$  nb/nucleon, which is consistent with recent NLO calculations.

## 1 Introduction

The measurement of bottom production in fixed target collisions offers the possibility to test perturbative QCD in the near threshold energy regime, where the effect of higher order processes, such as soft gluon emission, has been calculated [1, 2]. At first order, the production mechanism at the HERA-B energy ( $\sqrt{s} = 41.6$  GeV) is dominated by gluon-gluon fusion ( $gg \rightarrow b\bar{b}$ ) [3].

Three experimental results are published. Two are inconsistent, even though they were obtained by similar experiments searching for  $J/\psi$  [4] and semi-leptonic [5] decays of  $b$ -flavoured hadrons. HERA-B recently published the most accurate result based on a measurement of  $J/\psi$  decays of the  $b$ -flavoured hadrons [6].

In this paper, a measurement of the  $b\bar{b}$  production cross section performed with a  $b$  tagging technique independent from our previous measurement is presented.

After production,  $b\bar{b}$  pairs hadronise and mostly decay into  $c$ -flavoured hadrons. Since  $b$ -flavoured and  $c$ -flavoured hadrons have a large probability to decay with the emission of a muon (“semi-muonic decay”) [7], the  $b\bar{b}$  production cross section is measured by searching for  $b\bar{b} \rightarrow \mu\mu + X$  decay events, in which at least two of the four heavy quarks typically produced in a  $b\bar{b}$  event ( $b, \bar{b}, c, \bar{c}$ ) undergo semi-muonic decays (“double muonic  $b$  decays”).

The  $b\bar{b}$  event selection is based on a pair of oppositely charged muons not coming from the primary interaction vertex, having a large momentum transverse to the beam.

## 2 Detector and data sample

HERA-B [8, 9] is a large acceptance forward spectrometer installed at the 920 GeV proton storage ring of DESY. The Feynman- $x$  ( $x_F$ ) of accepted muons from semi-muonic  $b$  decays is between  $-0.3$  and  $0.15$ . The detector is used to reconstruct charged particle tracks produced in the interactions of the proton beam halo with wires of different materials ( $^{12}\text{C}$ ,  $^{48}\text{Ti}$  and  $^{184}\text{W}$ ), in several configurations [10]. Particles are tracked with a silicon microstrip detector [11] whose first station (of 8) is a few centimeters from the target system and which extends approximately 2 m further downstream. A primary vertex resolution of  $500 \mu\text{m}$  along the beam and  $50 \mu\text{m}$  in the perpendicular plane is achieved. Up to 13 m downstream of the target, honeycomb chambers

in the outer region [12, 13], and microstrip gaseous chambers in the inner region [14], allow to track particles and to measure their momenta from the bending in a 2.13 T·m vertical magnetic field. A Cherenkov detector [15] is used for  $\pi/K/p$  separation. An electromagnetic shashlik calorimeter [16] serves for  $e$  and  $\gamma$  identification. At the rear of the detector, muons with momenta larger than 5 GeV/ $c$  are tracked with triple stereo layers of gaseous tube chambers interleaved with hadron absorbers [17].

Double muonic  $b$  decays are searched for in  $164 \cdot 10^6$  events of  $p\text{-C}$ ,  $p\text{-Ti}$  and  $p\text{-W}$  interactions (1.4 overlapped interactions per event, in average) collected with a multilevel dilepton trigger [18] in the 2002-2003 data taking period. The trigger is designed to select dilepton decays of  $J/\psi$  mesons produced in the proton-nucleus collisions. By applying dimuon selection criteria similar to those of reference [6], about 146,000 prompt  $J/\psi$  mesons are reconstructed. With this event selection, double muonic  $b$  decays are a tiny fraction of the surviving muon pairs (Figure 1).

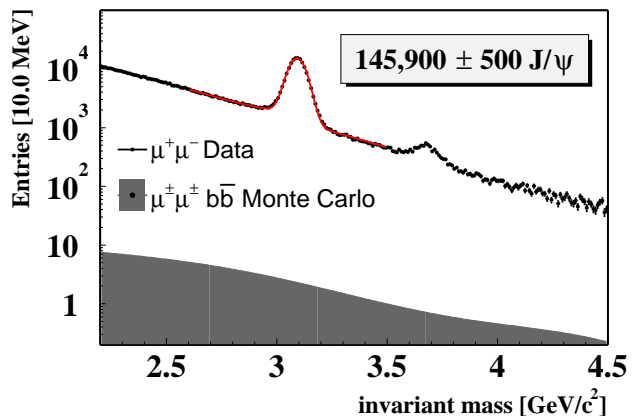


**Figure 1.** Invariant mass of opposite-sign muons after dimuon selection (white histogram). Two peaks emerge above the background ( $J/\psi$  and  $\psi'$ ). The fit of the  $J/\psi$  signal at  $3.097 \text{ GeV}/c^2$  (grey line) includes events in the radiative tail [19]. The grey histogram is a Monte Carlo simulation of double muonic  $b$  decays (see text for details).

The systematic uncertainties due to the detector performance and acceptance is reduced by normalising the  $b\bar{b}$  production cross section to the prompt  $J/\psi$  cross section.

### 3 Monte Carlo simulation

The acceptance and the reconstruction efficiencies are determined through Monte Carlo simulations of the physics processes occurring in proton-nucleus interactions. For bottom and charm production, PYTHIA 5.7 [20] is used. For bottom production, the predictions of NRQCD models are used, while  $J/\psi$  production is tuned to match the  $x_F$  and  $p_T$  distributions measured by other experiments. The fragmentation process is simulated by JETSET 7.4 [20]. The energy left from the hard scattering is used by FRITIOF [21] to simulate the underlying inelastic event. The response of the detector is simulated by GEANT 3.21 [22]. See, for more details, reference [6].

### 4 Measurement method

The  $b\bar{b}$  production cross section can be expressed as

$$\sigma_{b\bar{b}} = \frac{N_{b\bar{b}}^{+-} \Delta\sigma_{J/\psi} \text{BR}_{J/\psi}}{X_{b\bar{b}}^{+-}},$$

where  $N_{b\bar{b}}^{+-}$  is the total number of double muonic  $b$  decays in our  $\mu^+\mu^-$  sample,  $\Delta\sigma_{J/\psi} = 417 \pm 37$  nb/nucleon [23] is the prompt  $J/\psi$  production cross section in the detector acceptance ( $-0.35 < x_F(J/\psi) < 0.15$ ) and  $\text{BR}_{J/\psi}$  is the branching ratio for  $J/\psi \rightarrow \mu^+\mu^-$  decays ( $5.88 \pm 0.10\%$ ) [7]. The term  $X_{b\bar{b}}^{+-}$  is defined as

$$X_{b\bar{b}}^{+-} = \sum_i N_{J/\psi,i} A_i^{1-\alpha} \frac{\sum_j \text{BR}_{B_j} (1 - \theta_j) \varepsilon_{b\bar{b},j,i}^{+-}}{\varepsilon_{J/\psi,i}},$$

where the index  $i$  runs over 14 different target configurations. The index  $j$  refers to the different ways to generate dimuons via semileptonic  $b$  or  $b \rightarrow c$  decays (Section 5) having different branching ratios ( $\text{BR}_{B_j}$ ) and reconstruction efficiency ( $\varepsilon_{b\bar{b},j,i}^{+-}$ , the superscript indicates the dimuon charge). The charge factors  $\theta_j$  gives the fraction of resulting same-sign muons (Table 1),  $N_{J/\psi,i}$  is the number of  $J/\psi$  mesons reconstructed with efficiency  $\varepsilon_{J/\psi,i}$ ,  $A$  is the atomic weight of the target and  $\alpha = 0.96 \pm 0.01$  [24] is the  $J/\psi$  nuclear suppression in the central  $x_F$  region. Nuclear effects are expected to be negligible for open bottom and open charm production.

The number  $N_{b\bar{b}}^{+-}$  is obtained with two methods leading to two determinations of the  $b\bar{b}$  production cross section (Section 7).

### 5 Signal decay modes

The signal sample consists of events with two muons coming from semi-muonic decays of heavy quarks. Four heavy quarks are typically produced in a  $b\bar{b}$  event ( $b, \bar{b}, c, \bar{c}$ ). Depending on the type of hadrons decaying in the semi-muonic mode ( $b\bar{b}, bc+\bar{b}\bar{c}, b\bar{c}+\bar{b}c$  or  $c\bar{c}$ ), four classes ( $B_j$ ) of signal events are defined [25] (Table 1).

Class	Decaying hadrons	Branching ratio	$\theta$
$B1$	$b\bar{b}$	0.0084	0.187
$B2$	$bc+\bar{b}\bar{c}$	0.0160	0
$B3$	$b\bar{c}+\bar{b}c$	0.0156	0.742
$B4$	$c\bar{c}$	0.0081	0.315

**Table 1.** Branching ratios and charge factors  $\theta$  (see text for details) of four classes of double muonic  $b$  decays. The branching ratios are correlated and are affected by a relative uncertainty of 10%. The relative uncertainty on  $\theta$  is less than 1%.

For each class, the branching ratio for dimuon decays is obtained from the branching ratios for semi-muonic  $b$  and  $c$  decays reported in the PDG [7]. The fraction of decays into same-sign muons ( $\mu^\pm\mu^\pm$ ) is given by a charge factor  $\theta$ ,  $1-\theta$  being the fraction of decays into opposite-sign muons ( $\mu^+\mu^-$ ). The value of  $\theta$  is determined through Monte Carlo simulations and includes the effect of  $B^0$  and  $B_S$  mixing and all possible decay paths leading to muon pairs.

A fifth class, which is not included above, must be also considered. Events in which  $\mu^+\mu^-$  pairs originate from double muonic decay of  $c\bar{c}$  pairs from  $b \rightarrow c\bar{c}s + X$  decays represent 5.5% of the total signal events. These events are assigned to the class  $B2$ , which exhibits a similar final state. The systematic uncertainty corresponding to this choice is included in the branching ratio  $\text{BR}(b \rightarrow c\bar{c}s + X)$ .

Events with more than two muons might fall into more than one class. In order to avoid multiple counting of signal events, the calculated branching ratios in Table 1 include the probability that  $b$ -flavoured and  $c$ -flavoured hadrons do not decay into muons, and events are assigned to classes with a priority given by the order of classes in Table 1.

## 6 Background contributions

The main background for  $b\bar{b}$  event selection is made of events having two muon-like tracks not coming from the primary interaction vertex. Two sources of this type are considered: double muonic decays of  $c$ -flavoured hadrons and random combinations of muons from decay of low mass mesons (mainly pions and kaons). The latter background is referred to as ‘‘combinatorial background’’.

The Monte Carlo simulation shows that a cut around the  $J/\psi$  mass (between  $2.95 \text{ GeV}/c^2$  and  $3.25 \text{ GeV}/c^2$ ) removes background events from  $b \rightarrow J/\psi + X$  decays and prompt  $J/\psi$  decays. The  $J/\psi$  mass region is excluded to be also statistically independent from the measurement of  $b\bar{b}$  production cross section in [6], where  $b\bar{b}$  events are identified with  $J/\psi$  decays of the  $b$ -flavoured hadrons.

Muons from Drell-Yan events are at least 10 times less abundant than the combinatorial background in the invariant mass region of interest [26].

The number of background events from double muonic  $c$  decays ( $N_{c\bar{c}}^{+-}$ ) is determined through a Monte Carlo simulation normalised to the number of prompt  $J/\psi$  mesons reconstructed in the data. It can be expressed as

$$N_{c\bar{c}}^{+-} = \frac{\sigma_{c\bar{c}} \text{BR}_{c\bar{c}}}{\Delta\sigma_{J/\psi} \text{BR}_{J/\psi}} X_{c\bar{c}},$$

where  $\sigma_{c\bar{c}}$  is the charm cross section [27] ( $49 \pm 5 \text{ } \mu\text{b/nucleon}$  [28]),  $\text{BR}_{c\bar{c}} = \text{BR}(c \rightarrow \mu + X)^2 = (0.082 \pm 0.005)^2$  [7], and the term  $X_{c\bar{c}}$  is defined as

$$X_{c\bar{c}} = \sum_i N_{J/\psi,i} A_i^{1-\alpha} \frac{\varepsilon_{c\bar{c},i}}{\varepsilon_{J/\psi,i}},$$

The term  $\varepsilon_{c\bar{c},i}$  is the  $b\bar{b}$  selection efficiency for double muonic  $c$  decay events in the target configuration  $i$ .

The combinatorial background in the  $\mu^+\mu^-$  channel ( $N_{co}^{+-}$ ) is determined with  $\mu^\pm\mu^\pm$  data.

Muons from double muonic  $b$  decays do not come from the same decay vertex. However, the forward boost in fixed target collisions is such that tracks coming from two long lived particle decays are almost as close as those originating from a single particle decay. In double muonic  $b$  decays, the middle point of the segment of minimum distance between the two muons ( $pm\bar{d}$ ) is preferentially located downstream of the target, while the region upstream of the target is dominated by combinatorial background, in both  $\mu^+\mu^-$  and  $\mu^\pm\mu^\pm$  channels.

Assuming that the combinatorial background in the two final states has a similar shape, the number of events are normalised with respect to the upstream side and the combinatorial background in the  $\mu^+\mu^-$  channel is estimated as the difference between the number of  $\mu^\pm\mu^\pm$  pairs in data ( $N_{\mu\mu}^{\pm\pm}$ ) and those expected from double muonic  $b$  decays in the same channel ( $N_{b\bar{b}}^{\pm\pm}$ )

$$N_{co}^{+-} = N_{\mu\mu}^{\pm\pm} - N_{b\bar{b}}^{\pm\pm}.$$

$N_{b\bar{b}}^{\pm\pm}$  is obtained from Monte Carlo simulations, under the assumption that  $\sigma_{b\bar{b}} = 15 \text{ nb/nucleon}$ , with the formula

$$N_{b\bar{b}}^{\pm\pm} = \frac{\sigma_{b\bar{b}}}{\Delta\sigma_{J/\psi} \text{BR}_{J/\psi}} X_{b\bar{b}}^{\pm\pm},$$

where the term  $X_{b\bar{b}}^{\pm\pm}$  is defined as

$$X_{b\bar{b}}^{\pm\pm} = \sum_i N_{J/\psi,i} A_i^{1-\alpha} \frac{\sum_j \text{BR}_{B_j} \theta_j \varepsilon_{b\bar{b},j,i}^{\pm\pm}}{\varepsilon_{J/\psi,i}}.$$

The term  $\varepsilon_{b\bar{b},j,i}^{\pm\pm}$  indicates the reconstruction efficiency for double muonic  $b$  decays into  $\mu^\pm\mu^\pm$ .

## 7 Data analysis

Two methods have been used to estimate the number of events from  $b\bar{b}$  decay. A first method, which is used to obtain our final results, is described in Section 7.3 and a second method, which is used as a cross-check, is described in Section 7.4. With one exception (discussed below), the choice of cuts used in both methods is the same. Initial muon selection cuts are given in Section 7.1 and the procedure for optimizing the final cuts is described in Section 7.2.

The selection of  $b\bar{b}$  decay events begins by requiring that the events have at least two muons.

### 7.1 Muon selection

A first general muon selection is performed by requiring a high-quality reconstructed triggered track having a momentum between 5 and 200  $\text{GeV}/c$ , a minimum transverse momentum ( $p_T$ ) of 0.7  $\text{GeV}/c$  and a minimum  $\chi^2$  probability of the track fit ( $P_\chi$ ) of 0.003. The muon likelihood [29], as measured in the muon detector, must be greater than 0.05.

## 7.2 Cut optimisation

Both muons of an event are required to have a minimum  $p_T$  of 1 GeV/c and a minimum impact parameter to the target ( $Ip$ ) of  $1.5\sigma$  (where  $\sigma$  is the  $Ip$  resolution). The  $Ip$  is defined as the perpendicular distance between the target wire and the point on the track extrapolated to the  $z$ -position of the target. The dimuon invariant mass ( $m$ ) is required to be at least 2 GeV/c<sup>2</sup>.

The optimal  $b\bar{b}$  selection criteria are found by maximising the signal significance  $S$ , which is defined as

$$S = \frac{N_{b\bar{b}}^{+-}}{\sqrt{N_{b\bar{b}}^{+-} + N_{c\bar{c}}^{+-} + N_{c\bar{o}}^{+-}}}.$$

The number of signal events ( $N_{b\bar{b}}^{+-}$ ), which consists of oppositely charged muons, is obtained from Monte Carlo simulations, under the assumption that  $\sigma_{b\bar{b}} = 15$  nb/nucleon:

$$N_{b\bar{b}}^{+-} = \frac{\sigma_{b\bar{b}}}{\Delta\sigma_{J/\psi} \text{BR}_{J/\psi}} X_{b\bar{b}}^{+-}.$$

The formulae used to estimate the number of background events ( $N_{c\bar{c}}^{+-}$  and  $N_{c\bar{o}}^{+-}$ ) have been presented in Section 6.

A large fraction of combinatorial background consists of muonic decays of kaons and pions. Since the angle between the emitted muon and the decaying particle (kaon or pion) is small, such a background is suppressed by increasing the lower limit on  $P_\chi$ .

An upper limit on the kaon likelihood ( $L_k$ ) [30], as measured in the Cherenkov detector, suppresses muon candidates from kaon decays.

A lower limit on  $p_T$  suppresses muons from low mass particle decays, since they are expected to have a smaller  $p_T$  than those from  $b$  decays.

A lower limit on  $Ip$  discriminates muons originating in  $b$  decays from background muons. Since the  $Ip$  is correlated with the lifetime of the decaying particle, and the lifetime of  $b$ -flavoured hadrons is larger than that of  $c$ -flavoured hadrons, the impact parameter cut suppresses open charm background.

In order to suppress background in the proximity of the target, a lower limit on the difference between the  $pmd$  and the target positions along the  $z$ -axis ( $\Delta z$ ) is applied.

Unphysical events are suppressed by the requirement of the following upper limits:  $Ip < 50\sigma$ ,  $p_T < 5$  GeV/c,

$|\Delta z| < 5$  cm and  $m < 8$  GeV/c<sup>2</sup>. The optimisation of the last three cuts (lower limits on  $p_T$ ,  $Ip$  and  $\Delta z$ ) is performed simultaneously.

The optimisation procedure for  $S$  results in the  $b\bar{b}$  selection criteria listed in Table 2, where the number of surviving  $\mu^+\mu^-$  and  $\mu^\pm\mu^\pm$  pairs in the data, at each selection step, are also shown. After applying all cuts, the number of remaining dimuon candidates is

$$N_{\mu\mu}^{+-} = 167 \pm 13_{stat}.$$

Cut	$N_{\mu\mu}^{+-}$	$N_{\mu\mu}^{\pm\pm}$
High quality muon pairs	1051593	739947
$p_T > 1$ GeV/c, $Ip > 1.5\sigma$	34745	22359
$m \in [2, 8]$ GeV/c <sup>2</sup> , no J/ $\psi$	23560	19254
Upper limits	23406	19129
$P_\chi > 0.04$ , $L_k < 0.9$	16750	13268
$Ip > 4\sigma$	582	402
$\Delta z > 0.4$ cm	167	100

**Table 2.** Double muonic  $b$  decay selection and surviving  $\mu^+\mu^-$  and  $\mu^\pm\mu^\pm$  pairs in the data obtained from cut optimisation.

In the main measurement method, the  $\Delta z$  cut is relaxed to 0.2 cm (see Section 7.3). For this cut value, the resulting numbers of opposite-sign and same-sign muons are 225 and 117, respectively.

The invariant mass distribution of dimuon events surviving the  $b\bar{b}$  selection is shown in Figure 2 (the invariant mass cut on the J/ $\psi$  is removed for illustrative purposes).

## 7.3 Cross section determination

In the main measurement method, the number of  $b\bar{b}$  decay events in the data ( $N_{b\bar{b}}^{+-}$ ) is obtained from a likelihood fit to the data of the simulated  $p_T$  and  $Ip$  distributions of signal and background events. The selection criteria listed in Table 2 are applied, with the exception of the lower limit on  $\Delta z$ , which is decreased to 0.2 cm. The number of surviving  $\mu^+\mu^-$  pairs becomes

$$N_{\mu\mu}^{+-} = 225 \pm 15_{stat}.$$

The selection on  $\Delta z$  is relaxed because the likelihood fit uses more information than that used in the cut optimisation. The likelihood fit is also sensitive to the shapes

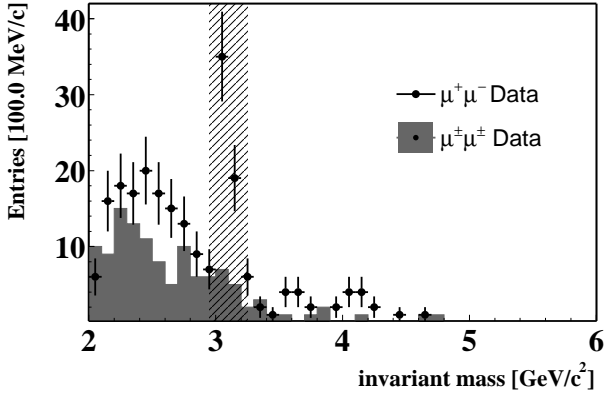


**Figure 2.** Dimuon invariant mass after  $b\bar{b}$  selection. Events in the  $J/\psi$  mass region ( $[2.95, 3.25]$   $\text{GeV}/c^2$ ), which is highlighted in the picture, are mostly due to  $b \rightarrow J/\psi + X$  decays. Since they are used in a different analysis [6], they are removed.

of signal and background distributions, while the cut optimisation only uses the number of signal and background events surviving the selection.

The likelihood function is defined as

$$L(n_s, n_b) = \frac{(n_s + n_b)^n e^{-(n_s + n_b)}}{n!} \prod_{i=1}^n \left( \frac{n_s P_s + n_b P_b}{n_s + n_b} \right).$$

The product index  $i$  runs over the  $n$  ( $= N_{\mu\mu}^{+-}$ ) selected dimuon events, the exponential term accounts for Poisson fluctuations of signal and background,  $n_s$  ( $= N_{bb}^{+-}$ ) and  $n_b$  ( $= N_{cc}^{+-} + N_{co}^{+-}$ ) are fit parameters representing the number of signal and background events in  $\mu^+\mu^-$  data,  $P_s$  and  $P_b$  are the products of the  $I_p$  and  $p_T$  probability distributions of the two muons for signal and background events, as obtained from the Monte Carlo simulations [25]:

$$P_s = C_s \cdot (R_s P_{B1} + P_{BX}) \quad \text{and} \\ P_b = C_b \cdot (R_b P_{c\bar{c}} + P_{co}).$$

The signal probability ( $P_s$ ) is the sum of probabilities from decays of class  $B1$  ( $P_{B1}$ ),  $B2$ ,  $B3$  and  $B4$  ( $P_{BX}$ ) with ratio  $R_s = 1$ . The background probability ( $P_b$ ) is obtained by adding the probability for charm and combinatorial events ( $P_{c\bar{c}}$  and  $P_{co}$ ) with  $R_b = 0.2$ . The probability ratios  $R_s$  and  $R_b$  are determined through Monte Carlo simulations. Constant factors ( $C_s$  and  $C_b$ ) are used to normalise the total probability to unity.

The result of the likelihood fit performed by minimising the quantity  $-2 \log L$  is shown in Figure 3. The minimum is obtained when  $n_s = 76 \pm 12$  and  $n_b = 149 \pm 15$ , which corresponds to the  $b\bar{b}$  production Cross section:

$$\sigma_{b\bar{b}} = 16.2 \pm 2.5_{stat} \text{ nb/nucleon}.$$

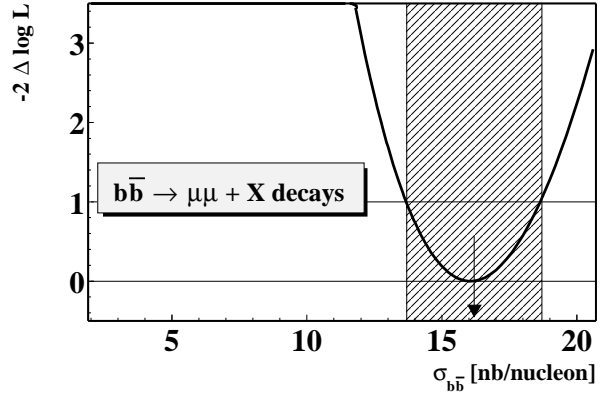


**Figure 3.** Dependence of  $-2\Delta \log L = -2(\log L - \log L_{min})$  on  $\sigma_{b\bar{b}}$ , where  $L$  is the likelihood of  $b\bar{b} \rightarrow \mu\mu + X$  decays. An increase of one unit on the vertical axis corresponds to a  $1\sigma$  variation of  $\sigma_{b\bar{b}}$ .

#### 7.4 Cross-check by a counting method

In a measurement method based on event counting,  $N_{bb}^{+-}$  is obtained by subtracting all possible background events from the number of  $\mu^+\mu^-$  pairs surviving the  $b\bar{b}$  selection listed in Table 2 ( $N_{\mu\mu}^{+-}$ ):

$$N_{bb}^{+-} = N_{\mu\mu}^{+-} - N_{c\bar{c}}^{+-} - (N_{\mu\mu}^{\pm\pm} - N_{bb}^{\pm\pm}).$$

Assuming that the reconstruction efficiency of  $b\bar{b}$  decays into  $\mu^+\mu^-$  is equal to that into  $\mu^\pm\mu^\pm$ , for each decay class in each target configuration ( $\varepsilon_{bb,j,i}^{\pm\pm} = \varepsilon_{bb,j,i}^{\pm\pm} = \varepsilon_{bb,j,i}^{\pm\pm}$ ), which is true to within a few percent, the  $b\bar{b}$  production cross section can be written as

$$\sigma_{b\bar{b}} = \frac{(N_{\mu\mu}^{+-} - N_{\mu\mu}^{\pm\pm}) \Delta\sigma_{J/\psi} \text{BR}_{J/\psi} - \sigma_{c\bar{c}} \text{BR}_{c\bar{c}} X_{c\bar{c}}}{X_{b\bar{b}}},$$

where the term  $X_{b\bar{b}}$  is given by

$$X_{b\bar{b}} = \sum_i N_{J/\psi,i} A_i^{1-\alpha} \frac{\sum_j \mathbf{BR}_{Bj} (1 - 2\theta_j) \varepsilon_{b\bar{b},j,i}}{\varepsilon_{J/\psi,i}}.$$

The number of dimuon events surviving the  $b\bar{b}$  selection are  $N_{\mu\mu}^{+-} = 167 \pm 13$  and  $N_{\mu\mu}^{\pm\pm} = 100 \pm 10$ . The simulated charm background is  $N_{c\bar{c}}^{+-} = 11.7 \pm 0.9$ , while the number of simulated  $b\bar{b}$  decays into same-sign muons are  $N_{b\bar{b}}^{\pm\pm} = 23 \pm 7$ . The resulting number of  $b\bar{b}$  decays into opposite-sign muons is  $N_{b\bar{b}}^{+-} = 78 \pm 23$  (the uncertainty takes into account the correlation between  $N_{b\bar{b}}^{+-}$  and  $N_{b\bar{b}}^{\pm\pm}$ ).

The result of the event counting method is the  $b\bar{b}$  cross section  $\sigma_{b\bar{b}} = 18.2 \pm 5.4_{stat}$  nb/nucleon.

Compared to the result of the likelihood fit, the statistical uncertainty is increased. This is due to the fact that the cross section is proportional to the difference between two numbers having a large statistical uncertainty ( $N_{b\bar{b}}^{+-} \propto N_{\mu\mu}^{+-} - N_{\mu\mu}^{\pm\pm}$ ), while, in the previous method,  $N_{b\bar{b}}^{+-}$  is obtained from  $\mu^+\mu^-$  data only. However, for the likelihood fit, the selection criteria are relaxed, which implies that the selected  $b\bar{b}$  events contain a larger fraction of background. The advantage is that the likelihood fit takes into account also the shapes of the signal and background distributions.

The likelihood fit is used to estimate the number of  $b\bar{b}$  events in the data, while the event counting method serves to estimate the systematic uncertainty associated with the measurement method.

## 8 Systematic uncertainty

Many systematic uncertainties on the measurement presented in this paper are similar to those reported in reference [6], where the reader can find a detailed discussion of detector and trigger simulations, models used to simulate  $b$ -flavoured hadron production and decay, production of  $J/\psi$  mesons, fluctuations of the proton-nucleus interaction rate, beam position and shape.

The reconstruction efficiency and the production cross section of  $J/\psi$  mesons are determined assuming no polarisation. The systematic uncertainty associated with  $J/\psi$  production includes the effect of a polarization consistent with the limits provided by other experiments [31, 32, 33].

The contributions specifically affecting the  $b\bar{b}$  cross section measurement from double muonic  $b$  decays are evalu-

ated. Those which are due to event selection are defined as the maximum variation of  $\sigma_{b\bar{b}}$ , divided by  $\sqrt{12}$ , obtained when varying crucial quantities in the likelihood fit, such as the impact parameter cut ( $Ip$ ) and the assumptions on signal and background composition ( $R_s$  and  $R_b$ ). The  $Ip$  cut is varied between 2 and  $6\sigma$ ,  $R_s$  in the range  $[0.5, 2]$  and  $R_b$  in the range  $[0, 0.4]$  (Figure 4).

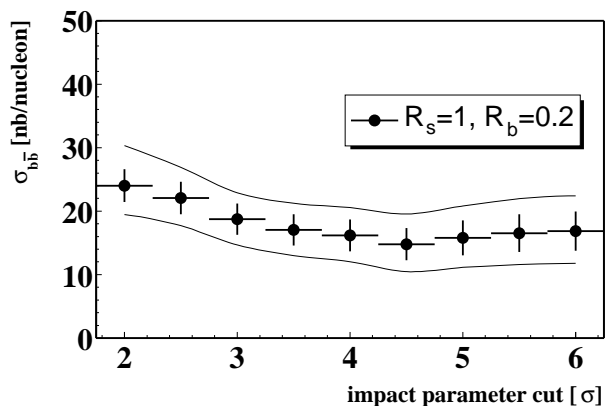


**Figure 4.** Dependence of the  $b\bar{b}$  production cross section on the muon impact parameter cut. The band represents the variation of cross section due to a change of the expected signal and background composition ( $R_s$  and  $R_b$ ) in the ranges  $[0.5, 2]$  and  $[0, 0.4]$ , respectively.

For cut optimisation (Section 7.2), a  $b\bar{b}$  cross section of 15 nb/nucleon is assumed. Since a variation of the value chosen for  $\sigma_{b\bar{b}}$  might result in a different event selection, the systematic uncertainty due to the assumption on  $\sigma_{b\bar{b}}$  is included in the effect of cut variation.

The systematic effect due to the measurement method is 6%. This effect is estimated by determining  $\sigma_{b\bar{b}}$  with the two methods described in Section 7 on the events surviving the  $b\bar{b}$  selection (Table 2).

The systematic effect due to the assignment of a priority to the classes of double muonic  $b$  decays is negligible.

Assuming that all uncertainties listed in Table 3 are independent, the total systematic uncertainty is 18%.

## 9 Conclusions

The  $b\bar{b}$  production cross section in 920 GeV proton-nucleus fixed target collisions has been measured by using double muonic  $b$ -flavoured hadron decays. The measurement is performed with a likelihood fit of the simulated kinemati-

Systematic effect	Uncertainty
Detector and trigger simulation	5%
$J/\psi$ production models	2.5%
$b\bar{b}$ production and decay models	5%
$b$ lifetime	1%
Proton-nucleus interaction rate	1%
Beam characteristics	0.5%
$\Delta\sigma_{J/\psi}$	8.9%
$\text{BR}(J/\psi \rightarrow \mu^+\mu^-)$	1.7%
$J/\psi$ nuclear suppression ( $\alpha$ )	3.7%
$J/\psi$ event counting	0.3%
Efficiency determination	2.0%
Charge factor ( $\theta$ )	0.3%
$\text{BR}(b \rightarrow \mu + X)$	3.5%
$\text{BR}(c \rightarrow \mu + X)$	3.2%
$\text{BR}(b \rightarrow c\bar{c}s + X)$	5.5%
$I_p$	5%
$R_s$ and $R_b$ ratios	6%
Measurement method	6%
<b>Total</b>	<b>18%</b>

**Table 3.** List of systematic effects in the measurement of  $\sigma_{b\bar{b}}$ . The first six contributions are evaluated in reference [6].

cal distributions of the signal and background events to the HERA-B dimuon data. The result is

$$\sigma_{b\bar{b}} = 16.2 \pm 2.5_{stat} \pm 2.8_{sys} \text{ nb/nucleon.}$$

The result is consistent with our previous measurement  $\sigma_{b\bar{b}} = 14.9 \pm 2.2_{stat} \pm 2.4_{sys} \text{ nb/nucleon}$  [6], which was performed on a statistically independent set of events. Both measurements are normalized to the prompt  $J/\psi$  production cross section.

The combined result of the two HERA-B measurements, accounting for the correlation between their systematic uncertainties, is

$$\sigma_{b\bar{b}} = 15.4 \pm 1.7_{stat} \pm 1.2_{sys}^{uncorr.} \pm 1.9_{sys}^{corr.} \text{ nb/nucleon,}$$

which is consistent with the latest QCD predictions of Bonciani *et al.* [1] and Kidonakis *et al.* [2] based on NLO calculations and resummation of soft gluons (Figure 5).

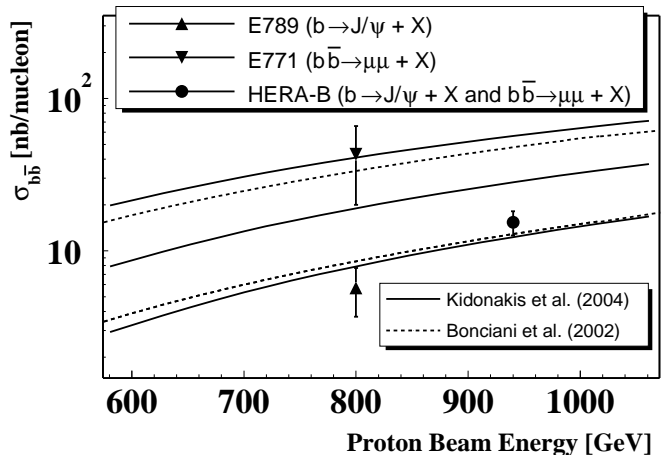


**Figure 5.** Cross section for  $b\bar{b}$  production as a function of the proton energy in fixed target collisions. The predictions of Bonciani *et al.* [1] and Kidonakis *et al.* [2] are shown. The theoretical uncertainties are obtained by changing the renormalisation and factorisation scales and the  $b$  mass. The HERA-B result, which is based on a combined analysis of  $b \rightarrow J/\psi + X$  and  $b\bar{b} \rightarrow \mu\mu + X$  decays, is consistent with the theoretical predictions. The results of the lower energy Fermilab experiments (E771 [5] and E789 [4]) are also shown.

## Acknowledgments

We thank F. Ferrolini for many stimulating discussions. We express our gratitude to the DESY laboratory and accelerator group for their strong support since the conception of the HERA-B experiment. The HERA-B experiment would not have been possible without the enormous effort and commitment of our technical and administrative staff.

## References

- [1] R. Bonciani *et al.*, Nucl. Phys. **B529** (1998) 424.
- [2] N. Kidonakis and R. Vogt, Eur. Phys. J. **C36** (2004) 201.
- [3] N. Kidonakis *et al.*, Phys. Rev. **D64** (2001) 114001.
- [4] D. M. Jansen *et al.*, Phys. Rev. Lett. **74** (1995) 3118.
- [5] T. Alexopoulos *et al.*, Phys. Rev. Lett. **82** (1999) 41.
- [6] I. Abt *et al.*, Phys. Rev. **D73** (2006) 052005.
- [7] W.-M. Yao *et al.*, J. Phys. **G33** (2006) 1.
- [8] T. Lohse *et al.*, DESY-PRC 94/02.
- [9] E. Hartouni *et al.*, DESY-PRC 95/01.

- [10] K. Ehret *et al.*, Nucl. Instrum. Meth. **A446** (2000) 190.
- [11] C. Bauer *et al.*, Nucl. Instrum. Meth. **A501** (2003) 39.
- [12] H. Albrecht *et al.*, Nucl. Instrum. Meth. **A541** (2005) 610.
- [13] H. Albrecht *et al.*, Nucl. Instrum. Meth. **A555** (2005) 310.
- [14] Y. Bagaturia *et al.*, Nucl. Instrum. Meth. **A490** (2002) 223.
- [15] I. Ariño *et al.*, Nucl. Instrum. Meth. **A516** (2004) 445.
- [16] G. Avoni *et al.*, Nucl. Instrum. Meth. **A461** (2001) 332.
- [17] A. Arefiev *et al.*, IEEE Trans. Nucl. Sci. **48** (2001) 1059.
- [18] V. Balagura *et al.*, Nucl. Instrum. Meth. **A494** (2002) 526.
- [19] A. Spiridonov, hep-ex/0510076 (unpublished).
- [20] T. Sjostrand, Comput. Phys. Commun. **82** (1994) 74.
- [21] H. Pi, Comput. Phys. Commun. **71** (1992) 173.
- [22] R. Brun *et al.*, Internal report CERN DD/EE/84-1 .
- [23] F. Maltoni *et al.*, Phys. Lett. **B638** (2006) 202.
- [24] M. J. Leitch *et al.*, Phys. Rev. Lett. **84** (2000) 3256.
- [25] A. Sbrizzi, Ph.D. thesis, NIKHEF, Amsterdam, 2006.
- [26] I. Abt *et al.*, Phys. Lett. **B638** (2006) 13.
- [27] C. Lourenço and H. K. Wöhri, Phys. Rept. **433** (2006) 127.
- [28] C. Lourenço and H. K. Wöhri, *private communication*.
- [29] M. Titov, Nucl. Instrum. Meth. **A446** (2000) 355.
- [30] M. Staric *et al.*, Nucl. Instrum. Meth. **A433** (1999) 279.
- [31] T. Alexopoulos *et al.*, Phys. Rev. **D55** (1997) 3927.
- [32] A. Gribushin *et al.*, Phys. Rev. **D62** (2000) 012001.
- [33] T. H. Chang *et al.*, Phys. Rev. Lett. **91** (2003) 211801.